SLAC-PUB-2107
April 1978
(T/E)

PARTICLE PRODUCTION IN A QUARK CASCADE MODEL*

A. Seiden and T. L. Schalk
University of California
Santa Cruz, California

and

J. F. Martin
Stanford Linear Accelerator Center
Stanford University, Stanford, California 94305

ABSTRACT

We compare measured hadron production in the quark fragmentation region with a simple quark cascade model. The comparisons test both the consistency of the data and the ability of a few simple assumptions to predict production probabilities for many different particle types.

(Submitted to Physical Review D)

*Work supported by the Department of Energy.

I. INTRODUCTION

We compare here a simple quark cascade model with a large body of recently available data from deep inelastic scattering reactions. In principle, the quark fragmentation hypothesis[1] is sufficient to allow a comparison of the data directly from these reactions, provided all final state hadrons are summed together. However, to predict the detailed distributions for various final state particles, given different initial quark mixtures, a model for the evolution of quarks into hadrons is needed. The comparisons presented here therefore not only test the quark fragmentation hypothesis as well as the consistency of the experimental data, they also test the ability of a few simple and universal assumptions to predict production probabilities for many different kinds of particles. More detailed data of the type discussed in this paper would help clarify the roles played by quark mass, hadron mass, and hadron spin in the production of hadrons in deep inelastic processes.

The principal assumptions of our quark cascade model, which is described in more detail in Ref. 2, are as follows:

1. The initial reaction yields a quark isolated in phase space.
2. The hadrons materializing in the fragmentation region of this isolated quark occur via a cascade of pairs produced from the vacuum as shown in Fig. 1. Each hadron generation comes from a quark q_i combining with a pair $q_j\bar{q}_j$, forming a meson $m = (q_j\bar{q}_j)$ and leaving a new quark q_j. This process repeats itself until a quark finally recombines with other quarks originating from the initial reaction.

3. The probability of finding a quark pair $q_j\bar{q}_j$, denoted by P_{q_j}, is assumed to be independent of the identity of q_i. As described in Ref. 2, we ignore high mass quarks and take for the P_{q_j} values suggested by particle ratios at high transverse momentum:

$q_j\bar{q}_j$	P_{q_j}
$u\bar{u}$	.4
$d\bar{d}$	.4
$s\bar{s}$	.2

The smaller value for the strange quark, a feature common to many quark-parton calculations, is a natural consequence of postulating that it has a larger mass. We shall look later at some data sensitive to these probabilities.

4. A pair $(q_i\bar{q}_j)$ yields a meson m with quantum numbers given by the quarks. We assume that mesons produced in this fashion lie wholly in the lowest-mass multiplet possible. Thus, if the $q_i\bar{q}_j$ helicities are opposite, we choose m to be a pseudoscalar meson; if the helicities are the same, we choose m to be a vector meson. This gives a vector to pseudoscalar ratio = 1. When several mesons in the multiplet contain $(q_i\bar{q}_j)$, the meson production probabilities are given by the appropriate SU(3) Clebsch-Gordon coefficients. The probability to produce a meson m from a quark q_i is called $C^m_{q_i}$, with $\sum_m C^m_{q_i} = 1$. Note that the production of baryons and heavy mesons is assumed to be small and is therefore ignored. With the above assumptions we can generate a table of $C^m_{q_i}$ for each quark as in Ref. 2. For example, for a u quark we get:

Pseudoscalar	C_u^m	Vector	C_u^m
π^+	.2	ρ^+	.2
π^o	.1	ρ^o	.1
η^o	.05	ω^o	.1
η'	.05	ϕ^o	.0
K^+	.1	K^{+*}	.1

These coefficients are again supported by particle ratios at high transverse momentum in hadron-hadron scattering.

5. In the process $q_i \to m + q_j$, where $m = (q_i\bar{q}_j)$, the energy of the initial quark is shared by the final meson and quark. In the high energy limit, this is assumed to happen in a scale invariant manner; that is, the probability for finding a meson with energy E_m depends only on $E_m/E_{q_i} = z_i$. The energy distribution in z_i is then specified by a function for each meson. We shall assume that this energy sharing function is independent of q_i and q_j. Thus, the probability of getting a meson m, with fractional energy z_i, at each step is given by $C_{q_i}^m\ f(z_i)$. The energy sharing function is normalized so that:

$$\int_0^1 f(z)dz = 1.$$

In Ref. 2, the simplest choice for the energy sharing function, $f(z) = 1$, was made. Since that time, considerably more data has appeared, indicating that a more complicated choice is necessary. We use some of the new data to fix $f(z)$ and then use our parametrization to make comparisons with the remaining data. A fundamental understanding of the form of the energy sharing function is as yet lacking.

A similar approach, with substantially the same assumptions as above, has been taken recently by Field and Feynman[3] who also provide some critical discussion of the assumptions involved. An exhaustive calculation of many properties of quark jets can be found there. Further recent work in this direction and some general results on multiplicity have been found by Sukhatme[4]. The inclusion of transverse momentum in this picture has been discussed in a simple way in Ref. 2. More general discussions on transverse momentum distributions can be found in Refs. 3 and 5, which make different assumptions and yield different conclusions.

II. ENERGY SHARING FUNCTION

We begin by listing several simple relations for the energy sharing function f(z). In the ideal situation, one would wish to measure this function in many ways, thereby checking that a unique function can really be used to describe the production of all the different mesons discussed. We assume below that the initial quark starting the cascade is a u quark which is a good approximation for neutrino-nucleon scattering, high Q^2 electron or muon-proton scattering. The full distribution for any meson m, summing over all production steps and after the decay of all resonances yielding m, is denoted by:

$$\frac{1}{\sigma_{tot}} \frac{d\sigma^m}{dz} = D_u^m(z), \text{ where } z = E_m/E_{max}.$$

E_{max} is the largest energy kinematically possible for m. This function grows with energy at small z since it is normalized to the multiplicity; therefore we shall usually consider instead the structure function:

$$F_u^m(z) = z\, D_u^m(z).$$

Integrating this over z we get the fraction of the available energy carried by mesons of type m. Scale invariance at each step for $f(z_i)$ translates into scale invariance for $F(z)$ as well as logarithmic growth with energy of total multiplicity.

A. Measuring f(z) Using Charged Vector Mesons

The initial cascade step leaves a quark mixture of u:d:s = 1:1:0.5. Within the cascade, the unit u to d ratio persists until the final recombination yielding a baryon. Therefore all charge differences are due to the first fragmentation step, although for π and K mesons, these differences are diluted by decays from heavier mesons. The ρ^+ and ρ^- mesons have an important advantage in that they get no contributions from the decay of heavier meson in this model; we see that f(z) can be directly measured as:

$$D_u^{\rho^+}(z) - D_u^{\rho^-}(z) = C_u^{\rho^+} f(z) = .2f(z).$$

Unfortunately, there are no data available on these at present, although they illustrate the usefulness of the subtracted distributions.

B. Measuring f(z) Using Neutral Vector Mesons

In this case, we again have the advantage that decays of heavier mesons do not complicate the distribution although we have to sum over many fragmentation steps. The result can be written in terms of integral equations as discussed in Ref. 4. In particular, we get a simple prediction for the structure function at z = 0:[4]

$$F_u^{\omega^o}(0) = F_u^{\rho^o}(0) = \left(\sum_i P_{q_i} C_{q_i}^{\rho}\right) I = (.08)I$$

$$F_u^{\phi^o}(0) = \left(\sum_i P_{q_i} C_{q_i}^{\phi}\right) I = (.02)I$$

where:

$$I = \left[\int_0^1 f(1-z)\ \ell n\ (\frac{1}{z})dz\right]^{-1} \quad .$$

This result is actually independent of which quark starts the cascade, as are the structure functions for any other meson at z=0. For any z, $F_u^{\omega^o}(z) = F_u^{\rho^o}(z)$, which would be particularly interesting to test in virtual photon initiated reactions. For these, vector dominance, at large z, predicts much different production ratios because of the coherent interference of the virtual pairs that the photon can dissociate into when yielding a vector meson. The Q^2 and z dependence for ρ^o and ω^o production would be a good probe of when coherent (diffractive) ideas are most appropriate and where incoherent (parton) ideas work best.

There are data available on the inclusive production of ρ^o mesons, although, because of the need to do complicated fits to di-pion mass distributions, the statistical errors here are fairly large. We therefore choose not to extract f(z) from that data, but will return to ρ^o distributions later.

C. Measuring f(z) Using Pion Distributions

The distribution for pions is complicated by contributions from heavier meson decays as well as the many fragmentation steps. We can, however, isolate the first cascade step by subtracting distributions as in the charged vector meson case. In particular, we can calculate the moments of the subtracted distributions in terms of those of the energy sharing function:

$$\int_{0}^{1}\left[D_u^{\pi^+}(z) - D_u^{\pi^-}(z)\right] dz = \left[C_u^{\pi^+} + C_u^{\rho^+} + \frac{2}{3}C_u^{K^{*+}}\right]\int_0^1 f(z)dz = .47.$$

$$\int_0^1\left[D_u^{\pi^+}(z) - D_u^{\pi^-}(z)\right] dz = \left[C_u^{\pi^+} + \left\langle\frac{z_\pi}{z_{\pi^+}}\right\rangle C_u^{\rho^+} + \left\langle\frac{z_{\pi^+}}{z_{K^{*+}}}\right\rangle\frac{2C_u^{K^{*+}}}{3}\right]\int_0^1 zf(z)dz$$

$$= .335\int_0^1 zf(z)dz \quad .$$

We shall use these relations to extract the energy sharing function assuming it can be parametrized in a simple way.

The data for the subtracted distributions are shown in Fig. 2.[6] These data are precise enough to allow a three parameter fit to f(z) of the form:

$$f(z) = a_1 + a_2(1-z) + a_3(1-z)^2 \quad .$$

We can find a_1 by noting that: $D_u^{\pi^+}(z \to 1) = a_1\, C_u^{\pi^+} = .2a_1$. To evaluate a_1, we use the muon scattering data of Fig. 8; the electron scattering data suffer from large radiative corrections (which are usually omitted) near z=1. The result is a_1 = .25, with an uncertainty of about 30%.

To solve for the remaining two coefficients, we will use the two moment relations listed above. In order to integrate over $D_u^{\pi^+} - D_u^{\pi^-}$, we follow Ref. 7 and use a parabola to describe this function. The properly normalized parabola is $D_u^{\pi^+} - D_u^{\pi^-} = .05 + 1.26\ (1-z)^2$, which has the correct integral of .47. This is shown as the dashed curve in Fig. 2, and indeed gives a good description of the data. We can multiply by $(.335)^{-1}z$ and integrate to get $\int_0^1 zf(z)dz = .38$; that is, the first meson generation carries on the average 38% of the initial quarks momentum. Solving for a_2 and a_3 gives then the curve in Fig. 3,

$$f(z) = .25 + 1.812(1-z) - .468(1-z)^2$$

with coefficients uncertain to roughly 20%. This is the level of accuracy we can expect in the comparisons to follow and, as we shall see, is the level of agreement of the various sets of experimental data themselves. Using the above f(z), we calculate $D_u^{\pi^+} - D_u^{\pi^-}$ using the model described earlier. The result is the solid curve in Fig. 2. The agreement is quite good and would be improved if radiative corrections, which amount to about 25% for the highest z points, were included in the data. The data also support the idea of the existence of a unique scale invariant function. Finally, for comparison, the dashed-dotted curve in Fig. 2 shows the prediction of Field and Feynman from Ref. 3, using f(z)=.23 + 2.31 (1-z) . Both this curve and other predictions from their model such as the pion structure function shown in Fig. 6 are quantitatively not very different from values we calculate.

III. COMPARISON WITH DATA

Given an initial quark type produced in a deep inelastic process, we can now calculate final state hadron distributions within the quark framentation picture. To simplify the calculation somewhat, we shall replace η' by the η^o everywhere in the calculation. This changes the distributions very little except for small changes in pion production near z=0. All calculations are performed assuming asymptotically high energies so as to give universal curves to compare to. Finite energy corrections are expected to change the results only at small z, provided energies are greater than a few GeV. We assume that pions from the decay of K_S^o and K_L^o are not included in the pion distributions. This is not true for all experiments, but again affects mainly the small z region.

A. Results for Charged Current Neutrino Reactions

The process $\nu(\bar{\nu})p \to \mu^-(\mu^+) + \pi^- + X$ results, in the parton model, nearly entirely from u(d) quark fragmentation. Choosing a final state negative particle avoids contamination from K^+ and protons and allows a good check for pion distributions. K^- contamination can be calculated to be very small (rising to a maximum of 20% at z=0). Thus the neutrino processes allow a comparison with the calculated structure functions $F_u^{\pi^+}(z) = F_d^{\pi^-}(z)$ and $F_u^{\pi^-}(z)$. The results are shown in Fig. 4.[8,9] The predictions are quite good; the data for $F_u^{\pi^+}$ shows perhaps a slightly steeper decrease with z than the curve. Figure 5 shows the model predictions for kaons of various types. These distributions have not as yet been measured.

B. Deep Inelastic Electron or Muon Scattering

For this case, the exact predictions depend on a knowledge of the quark content of the target nucleon. To avoid taking recourse to any specific model for the quark distributions in the nucleon, we shall choose structure functions to compare to which depend little on this detail. In particular, the distribution for $\pi^+ + \pi^-$ can be uniquely predicted if we ignore the presence of strange quarks in the sea, and the distribution for $K^+ + K^-$ can be predicted if we assume u quarks dominate the valence contribution and u, $\bar{u}$ quarks dominate the sea contribution. All of these assumptions are expected to be true since the photonic coupling for u and $\bar{u}$ quarks is four times larger than for the other quark types.

Distributions for $\pi^+ + \pi^-$, $K^+ + K^-$, and all charged hadrons are shown in Figs. 6, 7 and 8[10-13]. In plotting the data, we have ignored the difference between the two frequently used scaling variables z and x_F

since these are nearly equal at large values of either variable. The data for pions and all hadrons are in good agreement with the predicted curves which are expected to be accurate to about 20% based on the uncertainty in the energy sharing function. Data for charged kaon production considerably below the theoretical prediction. In the next section, we shall find that kaon production in e^+e^- annihilation agrees rather well with the theoretically calculated expectation. Whether this discrepancy would disappear at much higher Q^2 (the average value of $Q^2 = 1.2$ for the data in Fig. 7), or represents a serious deficiency in our ideas of universal quark fragmentation remains to be determined.

Finally, in Fig. 9 we present the distribution for the production of ρ^o mesons.[14] Although errors are large, ρ^o production is roughly as large as expected. Since the ρ^o is heavier than a kaon, the deficiency of kaons in Fig. 7 is probably not explainable purely as a mass suppression for kaons. Figures 10 and 11 show predictions for heavy mesons which have yet to be measured.

C. e^+e^- Annihilation

Data exists on the production of several particle types as well as all charged hadrons in this reaction. We restrict ourselves to energies where only the three light quarks contribute to the final state hadron distributions. In this case, the initial quark mixtures are: 2/3 $u\bar{u}$, 1/6 $d\bar{d}$, and 1/6 $s\bar{s}$. Figures 12 and 13 show the model predictions and data for final state pions and all charged hadrons,[15,16] respectively. The data on charged pions indicate a more rapid decrease with z in this reaction than predicted (and than in the lepto-production reactions), while the data for all hadrons show rough agreement with the prediction. This inconsistency between the two sets of data has yet to be resolved.

Figure 14 shows the predictions for charged and neutral kaons.[15,17,18] Again these data do not agree with the expectations from lepto-production data, but now do show reasonable agreement with the predicted curves. Particle production probabilities in this reaction do seem to be roughly consistent with the simple rules used. Note that, whereas the "flavor" dependence of the coupling for lepto-production yields large differences in production of π^+ and π^-, in the present reaction only the difference between charged and neutral kaons indicates that the final states "remember" the initial quark mixture produced. The differences at large z arise from the fact that u and $\bar{u}$ quarks yield mostly charged kaons. The data, unfortunately, are not precise enough to show a difference between charged and neutral kaon production.

Finally, if we take the predictions of the model seriously down to small z values, we can predict particle ratios in the central region provided events coming from charmed quarks or heavy leptons are identified and left out of the event sample. The rates are the same for all particles in a given isospin multiplet (except for small differences due to electromagnetic decays, such as $\omega^o \to \pi^o\gamma$), so we list only the neutral members:

Meson	$F_u^m(0)$
π^o	.65
K_S^o	.13
η^o	.08
ρ^o	.13
ϕ^o	.03
K^{*o}	.06

IV. CONCLUSIONS

We have shown that a simple quark cascade model successfully fits much of the data (π, K, ρ^o, at present) for final state hadron production in e^+e^- annihilation, $e(\mu)p$ deep inelastic scattering, and $\nu(\bar{\nu})p$ scattering. To predict the detailed distributions for each particle type, we have made assumptions about the effects of quark mass, hadron mass, and spin, which are simple and suggested by high transverse momentum particle ratios. The final ingredient, which we call the energy sharing function, has been extracted from the data on the difference of π^+ and π^- production from u quarks. If the data were available, this function could be measured in other ways which we have discussed. We have also presented predictions for the production of various meson types which have not yet been measured.

from u quarks. If the data were available, this function could be measured in other ways which we have discussed. We have also presented predictions for the production of various meson types which have not yet been measured.

REFERENCES

1. R. P. Feynman, Photon-Hadron Interactions (W. A. Benjamin, Reading, Mass., 1972).
2. A. Seiden, Phys. Lett. 68B, 157 (1977), and SLAC-PUB-1962 (1977).
3. R. D. Field and R. P. Feynman, Caltech preprint CALT-68-618 (1977).
4. U. P. Sukhatme, University of Cambridge preprint DAMTP 77/25 (1977), and Orsay preprint LPTHE 77/38 (1977).
5. Y. Zarmi, Weizmann Institute of Science preprint WIS-77/39-Ph (1977).
6. C. J. Bebek et al., Phys. Rev. D16, 1986 (1977).
7. L. M. Sehgal, Aachen preprint 77-0853 (1977).
8. M. Derrick et al., Argonne Nat'l Laboratory preprint ANL-HEP-PR-77-39.
9. B. P. Roe, Bubble Chamber Neutrino Results from Fermilab, Proc. of the 1975 Int. Symp. on Lepton and Photon Interactions at High Energies, Stanford, California.
10. We thank the members of the SLAC-MIT collaboration, of which one of us is a member (J.F.M.), for the use of their data. An extensive paper of their data is currently in preparation.
11. Ch. Berger et al., Phys. Lett. 70B, 471 (1977). The average Q^2 for these data is 0.9 $(GeV/c)^2$.
12. W. A. Loomis et al., "Hadron Production in Muon-Proton and Muon-Deuteron Collisions," to be published in Phys. Rev.
13. C. del Papa et al., SLAC-PUB-1965 (1977).
14. C. del Papa et al., Phys. Rev. Lett. 40, 359 (1977).
15. R. Brandelik et al., Phys. Lett. 67B, 359 (1977).

16. G. Feldman and M. Perl, Phys. Rep. 33C, 285 (1977), and Phys. Rep. 19C, 233 (1975).

17. V. Lüth, SLAC-PUB-2050 (1977).

18. J. Burmester et al., Phys. Lett. 67B, 367 (1977).

FIGURE CAPTIONS

1. q_1 is the initial quark yielded in the reaction. It combines with $\bar{q}_2$ to yield a meson, q_2 combines with $\bar{q}_3$, and so on.
2. The data are from Ref. 6. The curves result from our fit to these data points (see text). Dash-dotted curve comes from model in Ref. 3.
3. This curve is the energy sharing function found by the method described in the text. The coefficients are determined by fitting to the data in Fig. 2 only.
4. Comparison of the predicted shape for the pion structure functions with data from νp (filled circles, Ref. 9) and $\bar{\nu}p$ (open circles, Ref. 8).
5. Prediction of kaon structure functions for νp interactions.
6. Comparison of the predicted shape for the sum of π^+ and π^- with data from ep (Ref. 10) in which the contribution from elastic ρ^o has been subtracted. Shown also is the data for π^o production in ep (Ref. 11), which has been multiplied by 2 here for easy comparison. Dashed curve uses model from Ref. 3.
7. Comparison of the predicted shape for the sum of K^+ and K^- with data from ep (Ref. 10). Here data from hydrogen and deuterium targets has been combined.
8. Comparison of the predicted shape for the sum of h^+ and h^- (all charged hadrons) with data from ep, $\mu p(\mu n)$. The open circles are for data summed over hydrogen and deuterium (Ref. 13), the triangles are for $Q^2 \geq 2$ only, summed over hydrogen and deuterium (Ref. 12), and the filled circles are for hydrogen only. In all data the elastic ρ^o is subtracted (Ref. 10).
9. Comparison of the predicted shape for ρ^o with data from μp and μd (Ref. 14).

10. Prediction of structure functions for inclusive production of ρ^+, ρ^o, ρ^-, and ϕ^o mesons in ep or μp interactions at very high Q^2.

11. Prediction of structure functions for inclusive production of K^{*+}, K^{*-}, and η^o mesons in ep or μp interactions at very high Q^2.

12. Comparison of the predicted shape for π^+ or π^- from e^+e^- annihilation with data from Ref. 15.

13. Comparison of the predicted shape for h^+ or h^- from e^+e^- annihilation with data from Ref. 16.

14. Comparison of the predicted shapes for K^+ and K_S^o from e^+e^- annihilation with data from References 15 (filled circles), 17 (triangles), and 18 (squares). The K_S^o data of Ref. 17 were taken above charm threshold, but we expect no charm contribution for $z > 0.5$.

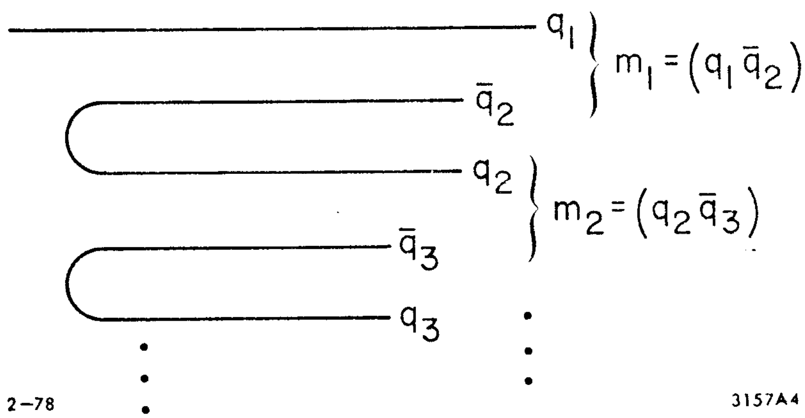

Fig. 1

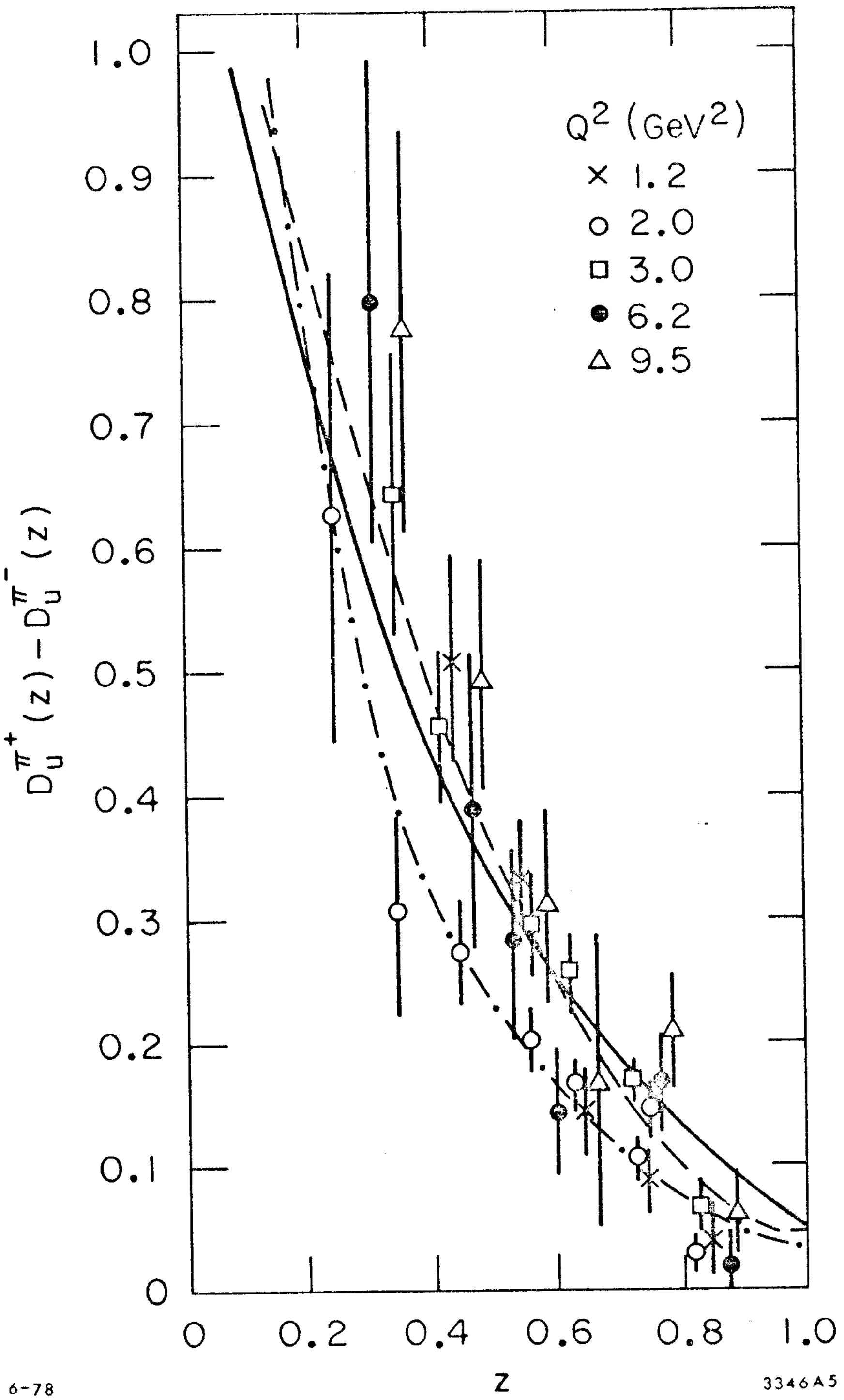

Q^2 (GeV^2)
× 1.2
○ 2.0
□ 3.0
● 6.2
△ 9.5
1.0
0.9
0.8
0.7
0.6
0.5
0.4
0.3
0.2
0.1
0
0.2
0.4
0.6
0.8
1.0
$D_u^{\pi^+}(z) - D_u^{\pi^-}(z)$
z
6-78
3346A5

Fig. 2

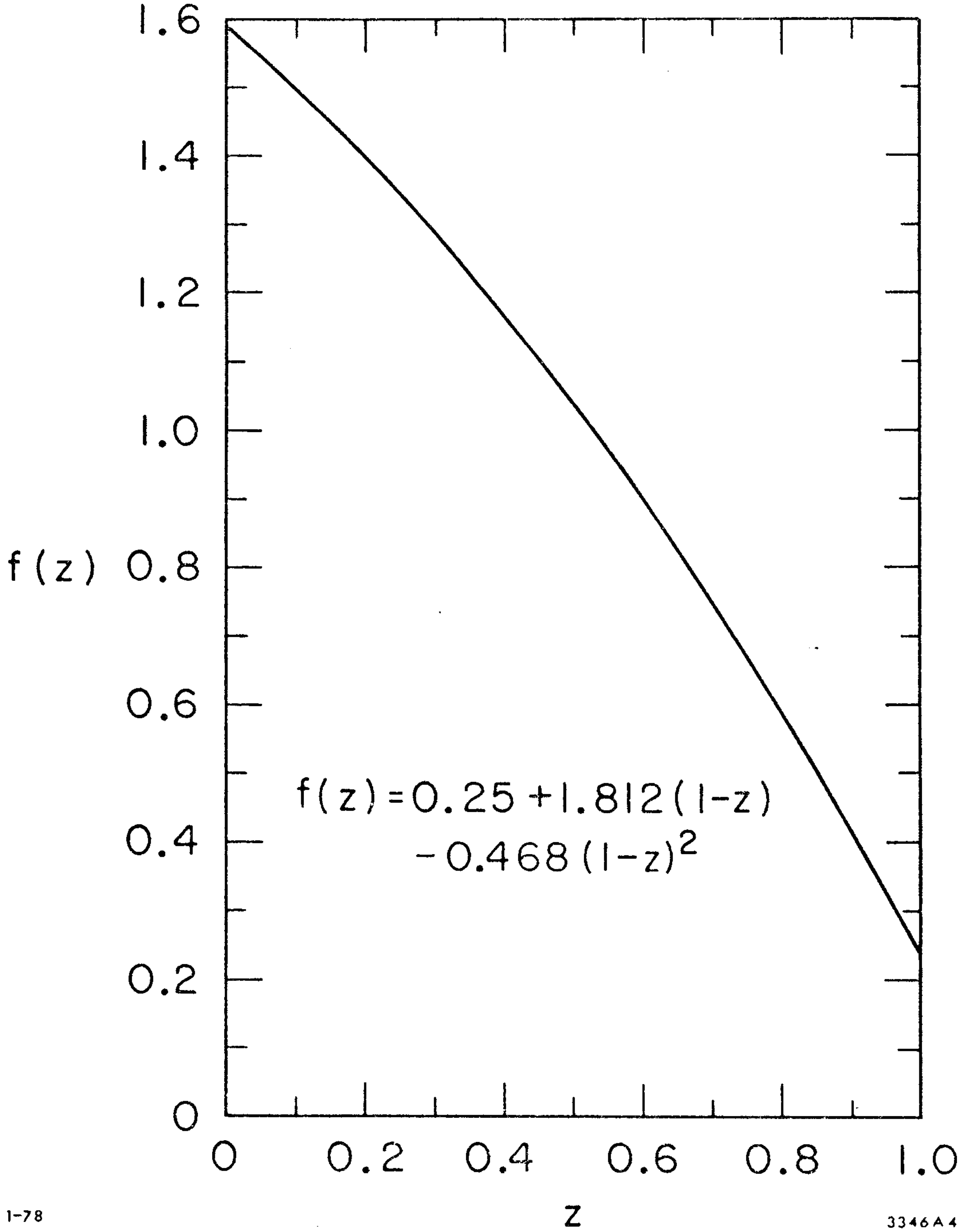
1.6
1.4
1.2
1.0
f(z) 0.8
0.6
0.4
0.2
0
0
0.2
0.4
0.6
0.8
1.0
z
f(z)=0.25+1.812(1-z)
-0.468(1-z)²
1-78
3346A4

Fig. 3

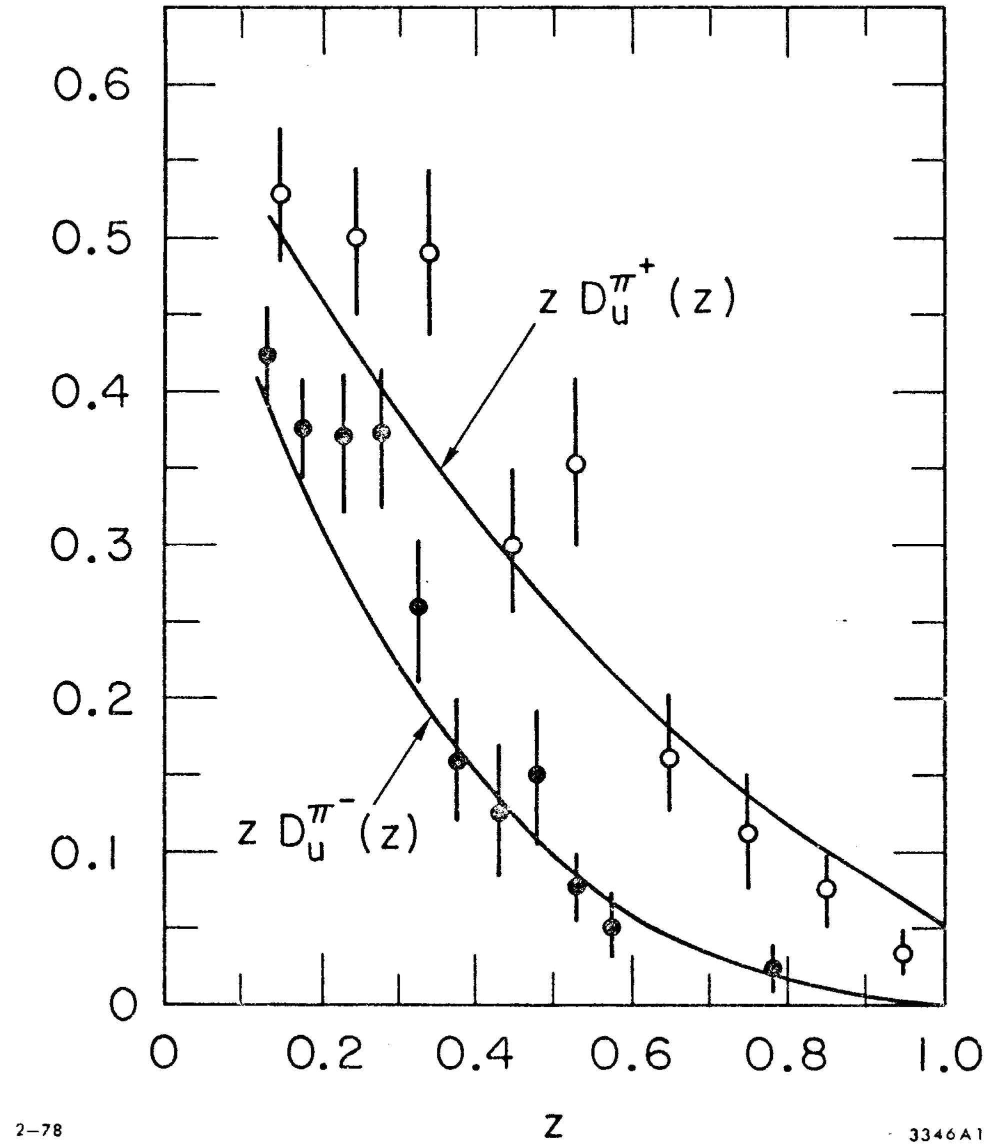

Fig. 4

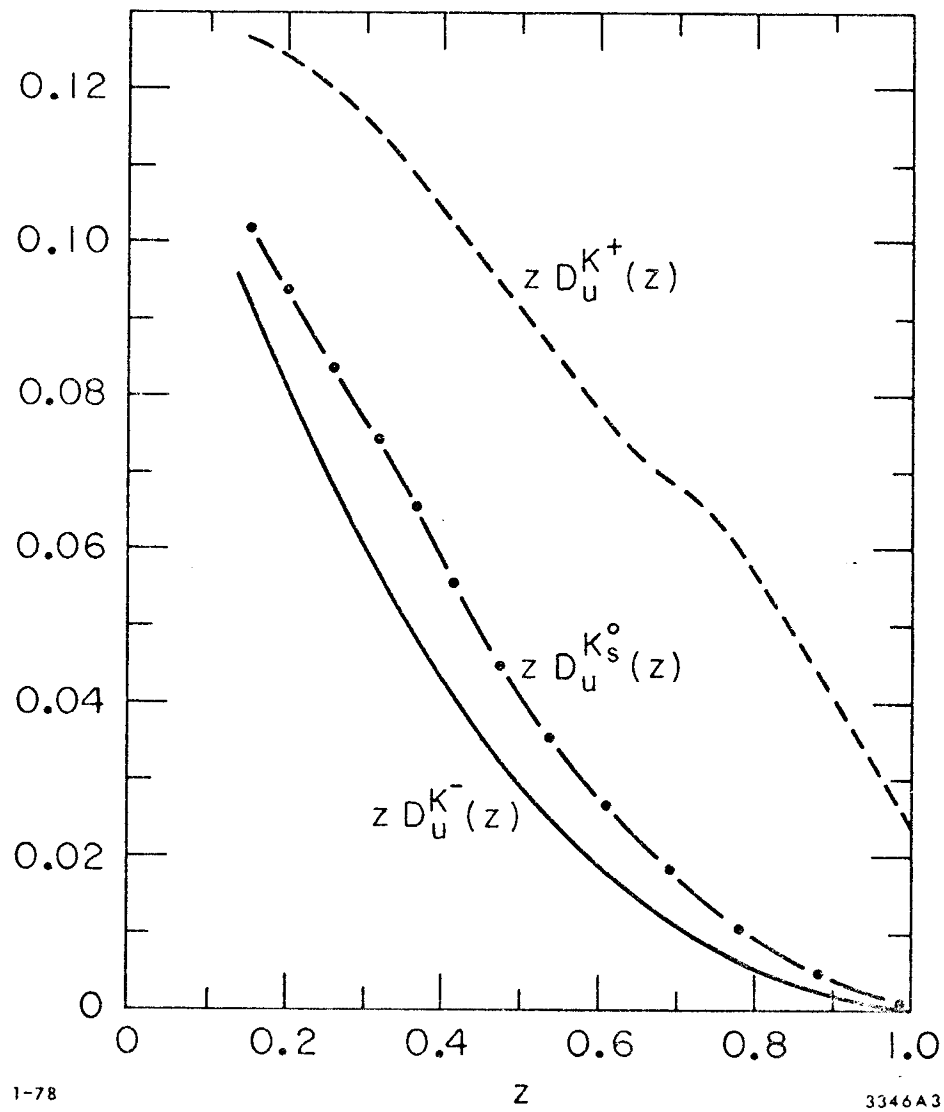
0.12
0.10
0.08
0.06
0.04
0.02
0
0
0.2
0.4
0.6
0.8
1.0
z
1-78
3346A3
z D u K+ (z)
z D u Ks° (z)
z D u K− (z)

Fig. 5

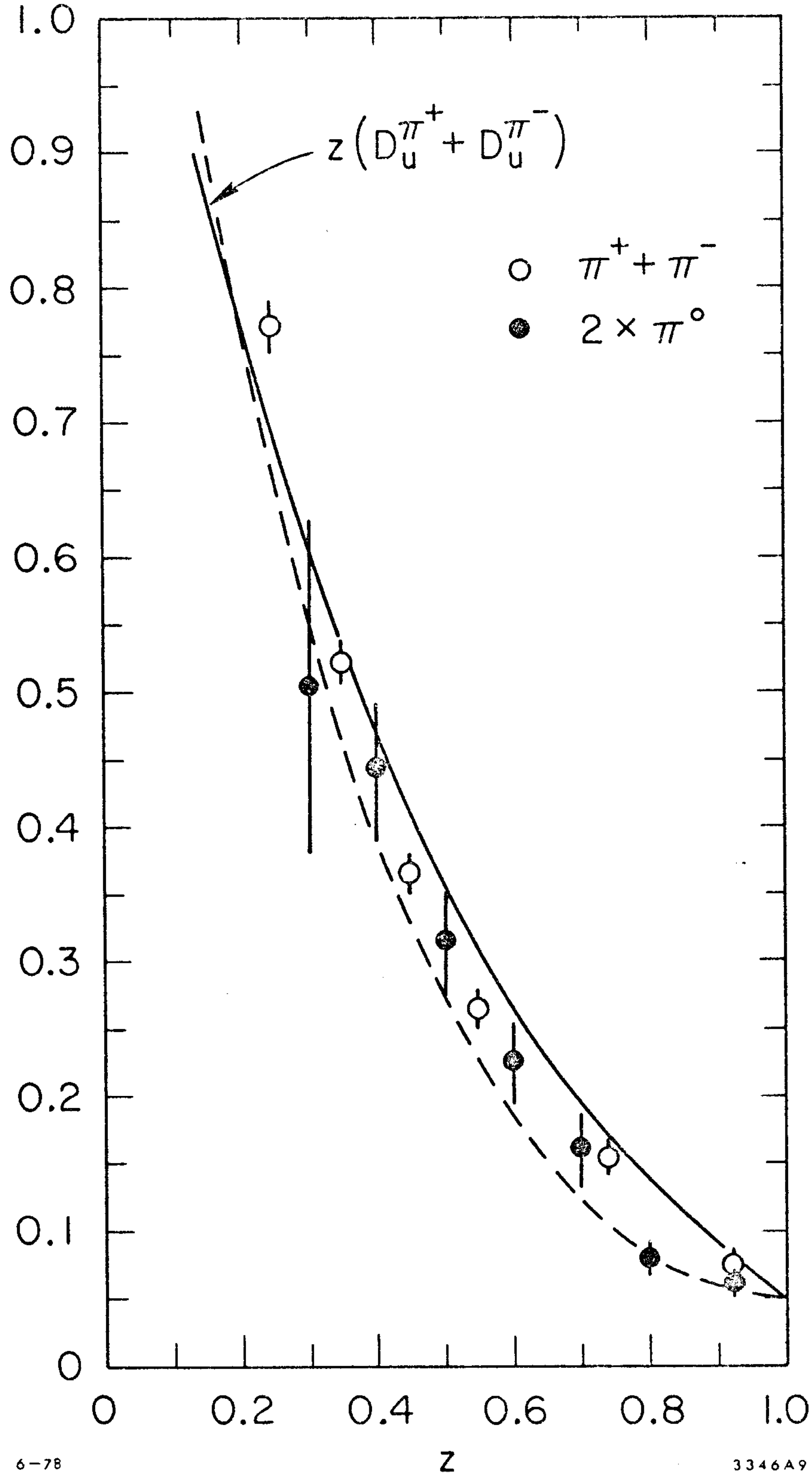

1.0
0.9
0.8
0.7
0.6
0.5
0.4
0.3
0.2
0.1
0
$z\left(D_u^{\pi^+} + D_u^{\pi^-}\right)$
$\pi^+ + \pi^-$
$2 \times \pi^\circ$
0
0.2
0.4
0.6
0.8
1.0
6-78
z
3346A9

Fig. 6

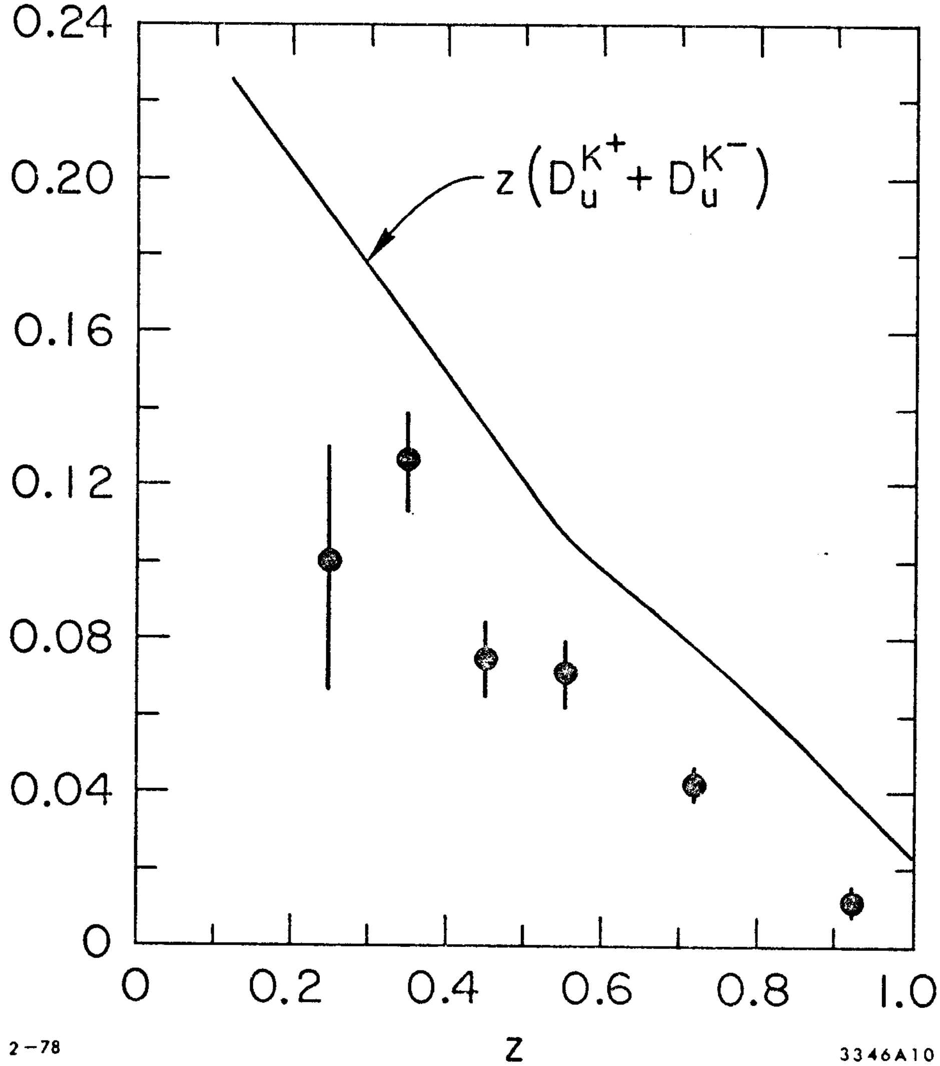

0.24
0.20
0.16
0.12
0.08
0.04
0
$z\left(D_u^{K^+} + D_u^{K^-}\right)$
0
0.2
0.4
0.6
0.8
1.0
2-78
z
3346A10

Fig. 7

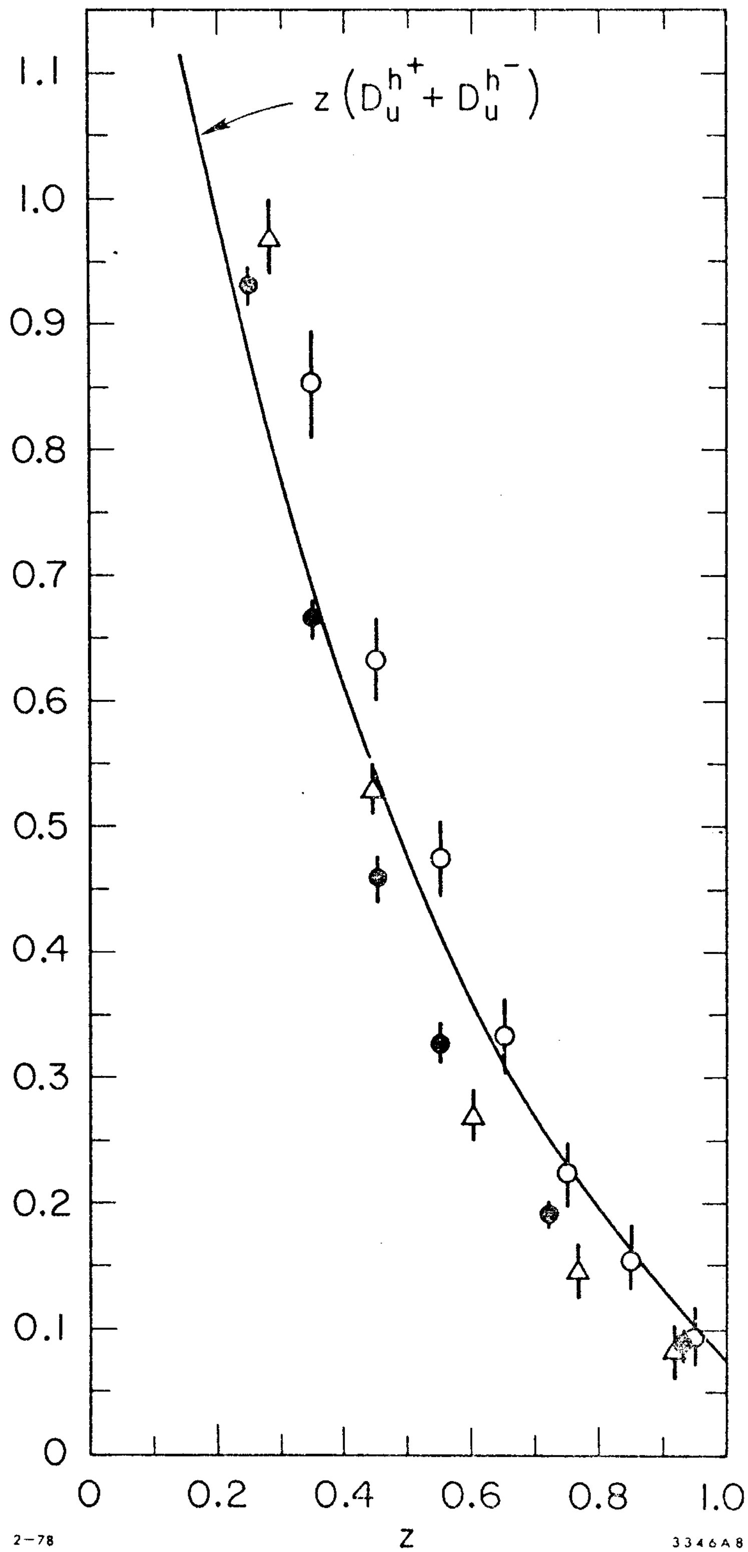

$z\left(D_u^{h^+} + D_u^{h^-}\right)$
1.1
1.0
0.9
0.8
0.7
0.6
0.5
0.4
0.3
0.2
0.1
0
0
0.2
0.4
0.6
0.8
1.0
2-78
z
3346A8

Fig. 8

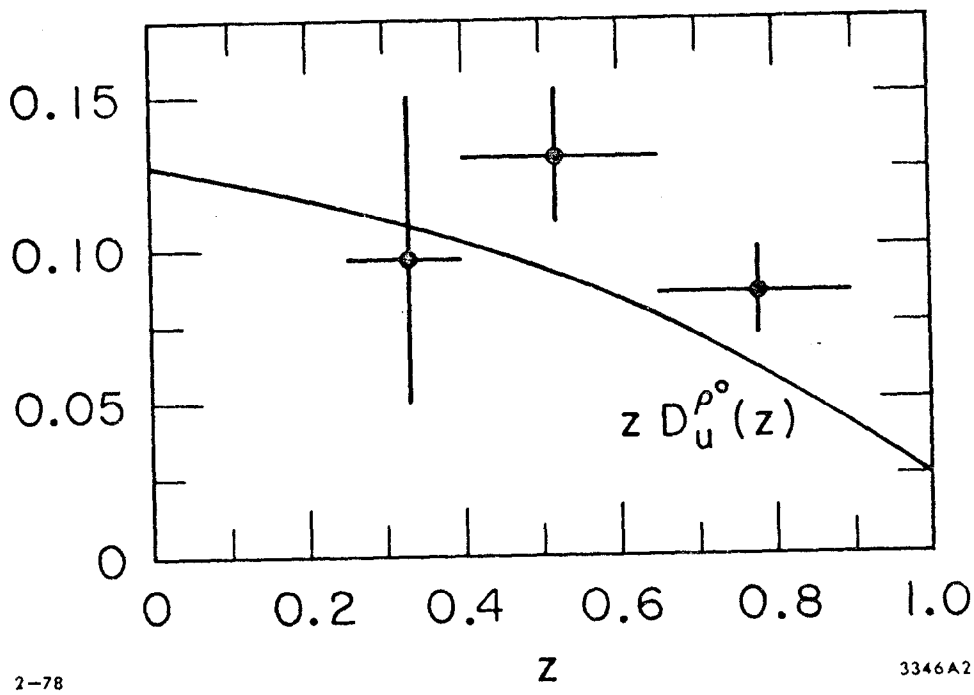

Fig. 9

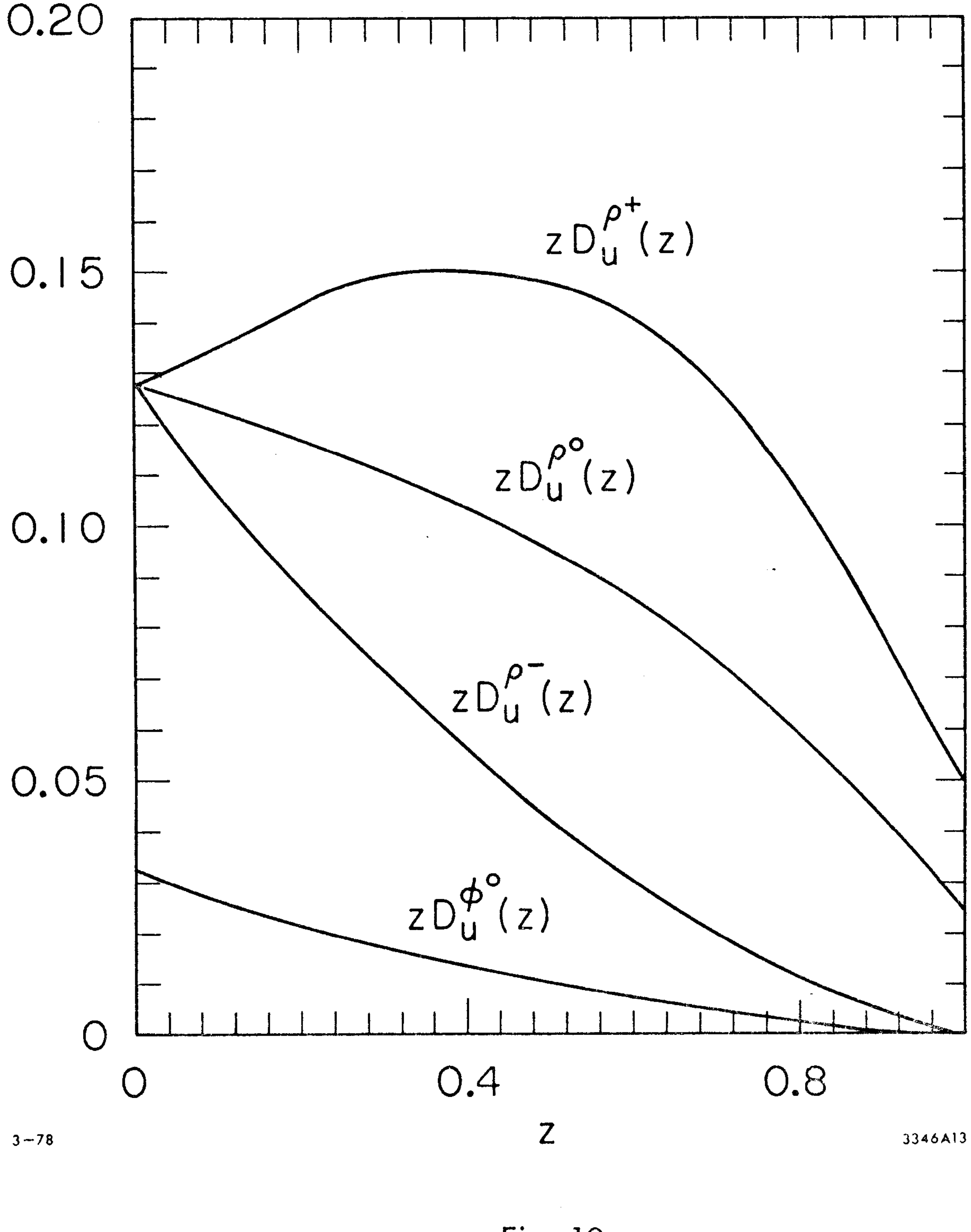

0.20
0.15
0.10
0.05
0
$zD_u^{\rho^+}(z)$
$zD_u^{\rho^0}(z)$
$zD_u^{\rho^-}(z)$
$zD_u^{\phi^0}(z)$
0
0.4
0.8
z
3-78
3346A13

Fig. 10

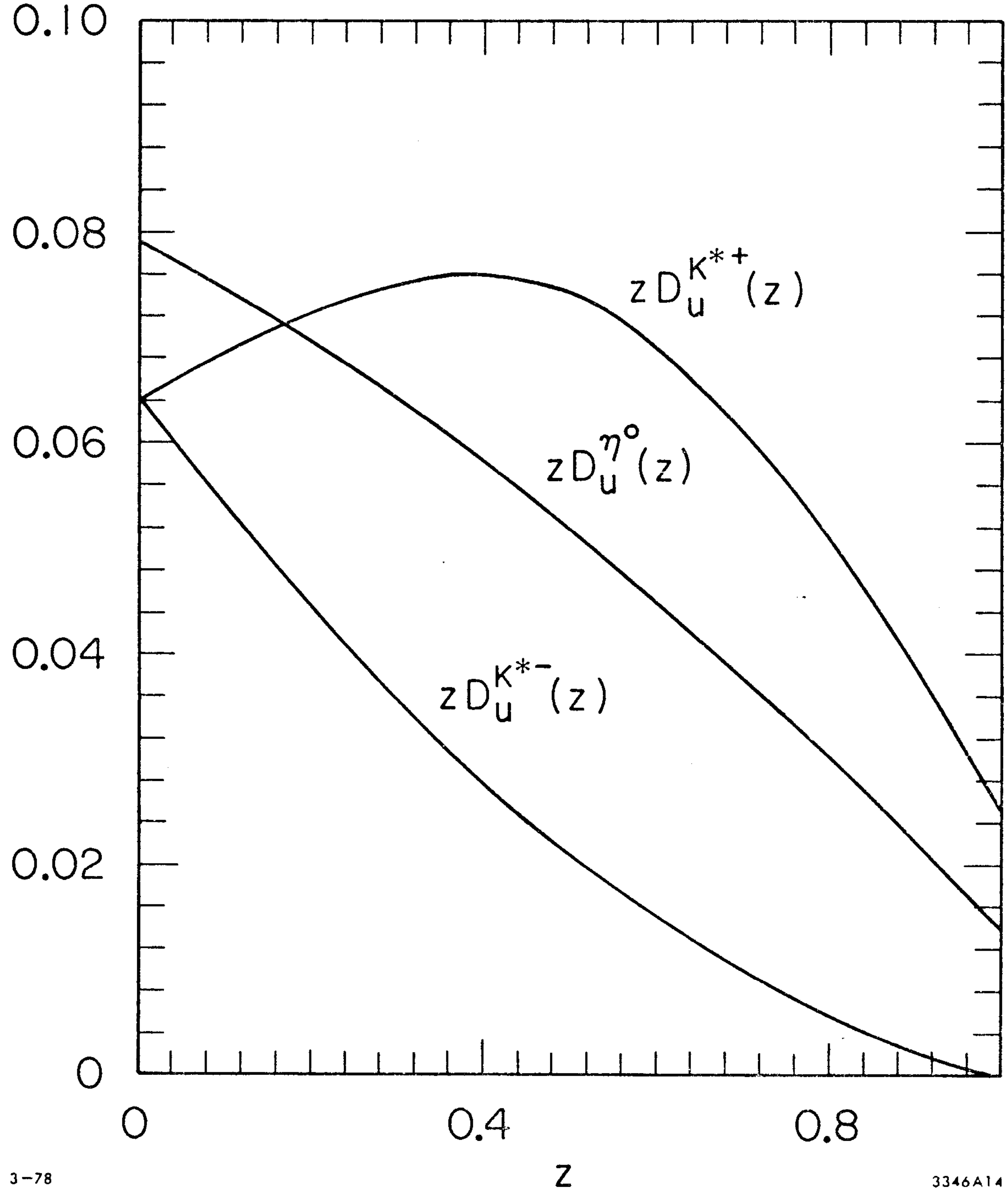

0.10
0.08
0.06
0.04
0.02
0
$zD_u^{K^{*+}}(z)$
$zD_u^{\eta^0}(z)$
$zD_u^{K^{*-}}(z)$
0
0.4
0.8
3-78
z
3346A14

Fig. 11

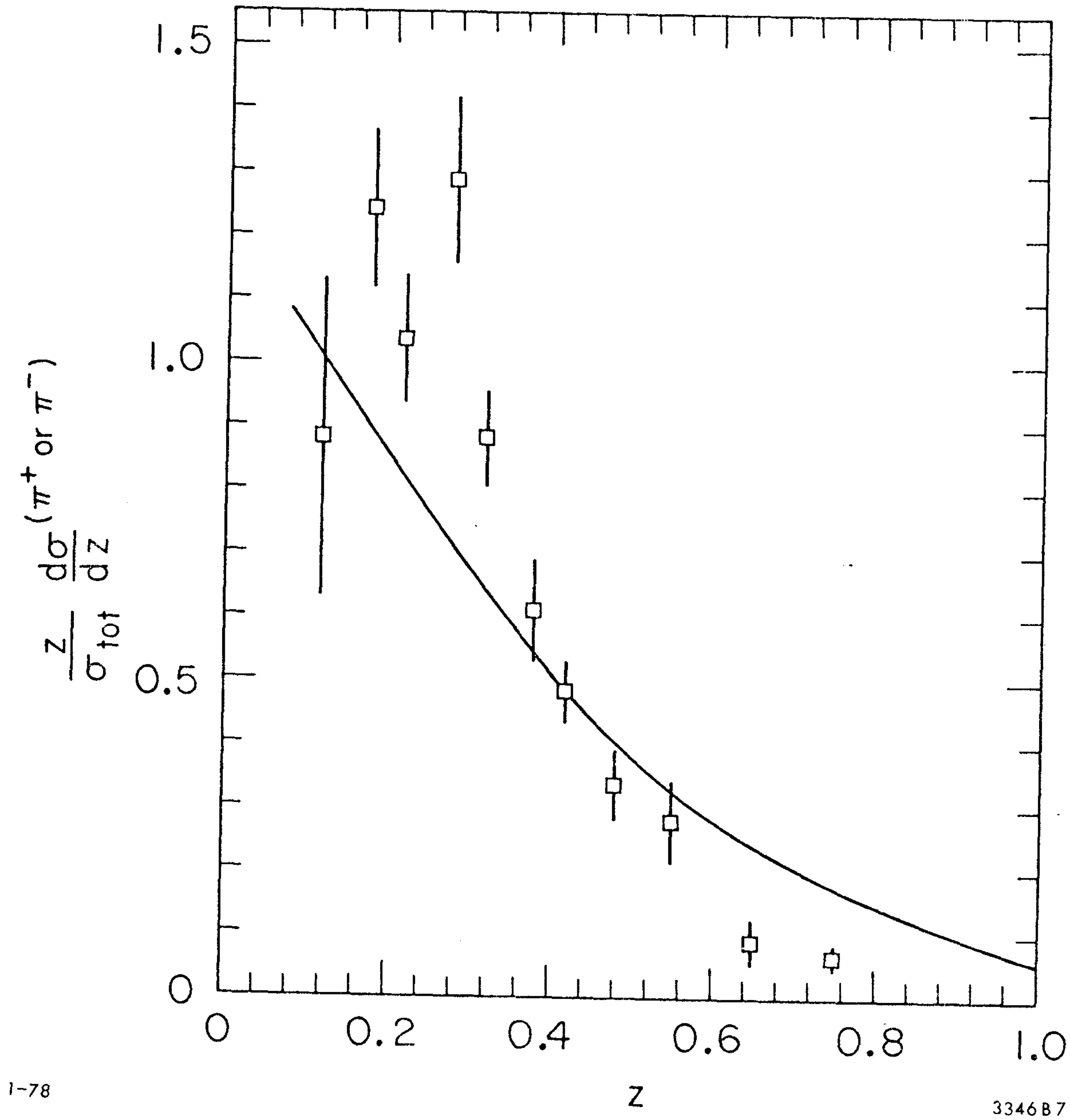
1.5
1.0
0.5
0
0
0.2
0.4
0.6
0.8
1.0
$\frac{z}{\sigma_{tot}} \frac{d\sigma}{dz}(\pi^+ \text{ or } \pi^-)$
z
1-78
3346B7

Fig. 12

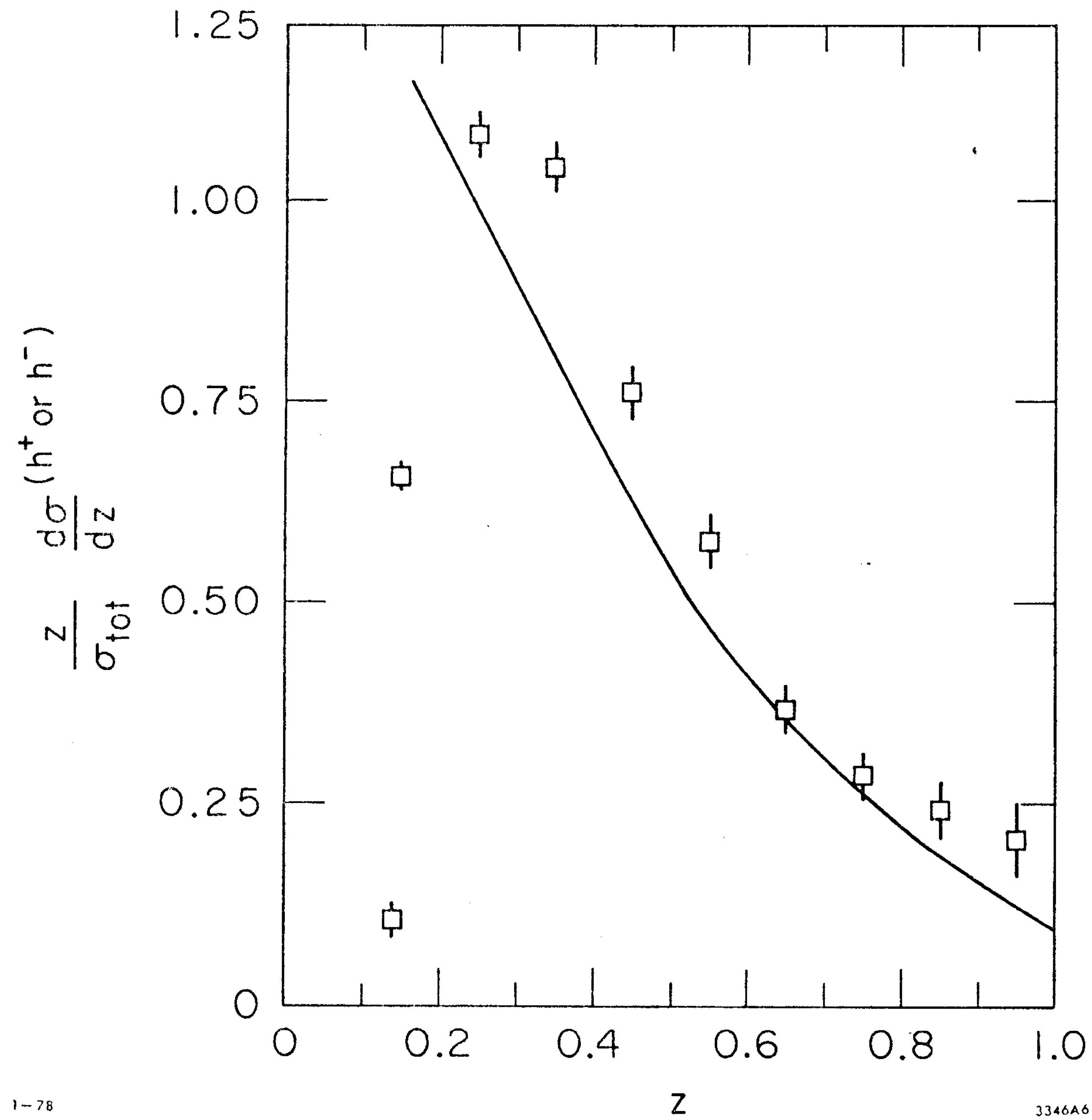
1.25
1.00
0.75
0.50
0.25
0
$\frac{z}{\sigma_{tot}} \frac{d\sigma}{dz}(h^+ \text{or } h^-)$
0
0.2
0.4
0.6
0.8
1.0
z
1-78
3346A6

Fig. 13

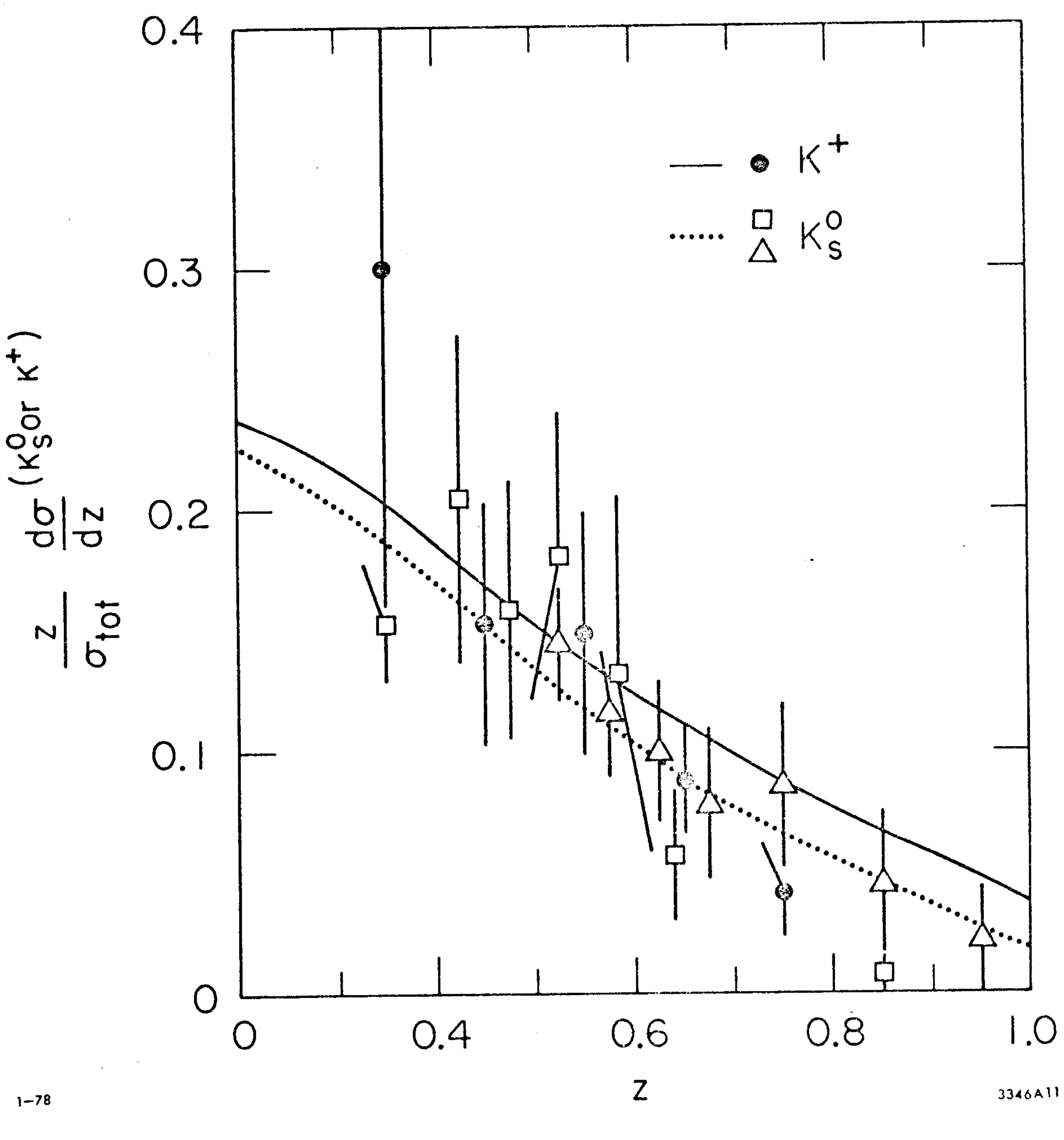
0.4
0.3
0.2
0.1
0
$\frac{z}{\sigma_{tot}} \frac{d\sigma}{dz} (K_S^0 \text{ or } K^+)$
K^+
K_S^0
0
0.4
0.6
0.8
1.0
z
1-78
3346A11

Fig. 14